ARTICLE NO. 79-0355R

J80-035

Influence of Chemical Kinetics and Unmixedness on Burning in Supersonic Hydrogen Flames

20014
60003
90011

John S. Evans* and Charles J. Schexnayder Jr.*
NASA Langley Research Center, Hampton, Va.

Good agreement has been obtained between published profiles of composition and pitot pressure with the calculated results from a computer program in which finite rate chemistry was used. Significant differences are noted between results calculated using 7 species and 8 reactions and those calculated using 12 species and 25 reactions. Differences are also found between results in which the effect of unmixedness on reaction in turbulent flow is applied or is not applied.

Introduction

MULTI-REACTION finite-rate chemistry has been used for many years in computer simulation of complex flowfields, and results have been good in laminar flows. Mixing of fuel and air is faster in turbulent flows than in laminar flows, but in turbulent flows the folding together of large volumes of fluid alternately rich in either fuel or oxygen produces the phenomenon of "unmixedness" in which the time-averaged temperature and composition at a point do not represent correctly the degree to which fuel and air are mixed on a molecular scale. Thus, the use of time-averaged values of temperatures and concentrations in the finite-rate chemistry equations is incorrect and can lead to serious errors in calculated results. This by no means rules out the use of time-averaged values, since the effects of unmixedness may be small for many turbulent, reacting flows. One purpose of this paper is to demonstrate that this is so by calculating some results with and without the effects of unmixedness. Another purpose of the paper is to report improvement in the ability of a computer program to simulate burning of H_2 in a supersonic air stream when an eddy breakup chemistry model is replaced with one in which finite reaction rates, corrected for unmixedness, are used.

In a prior investigation,[1] the usefulness of a parabolic marching computer program was evaluated by comparing computed results with data from five experimental test cases. Mixing of fuel and oxidant was computed for parallel injection of H_2 using a two-equation turbulence model, and the extent of chemical reaction was deduced by comparing the data with results obtained from three different assumptions: 1) no reaction, corresponding to zero combustion efficiency; 2) complete burning of all fuel mixed with oxygen, corresponding to combustion efficiency = 1; and 3) finite-rate burning based on the rate of decay of large turbulent eddies into small ones. The last of these assumptions, the eddy-breakup (EBU) model,[2] provided a means for obtaining combustion efficiency values intermediate between 0 and 1 and is believed to be useful as a tool to account for the effects of unmixedness on chemical reaction in turbulent flows if chemical reaction rates are large enough so that the production of combustion products is limited by the mixing rate.

In this paper three of the experimental test cases used in the previous computer program evaluation are reanalyzed using the same program but with a finite-rate chemistry system reported by Spiegler.[3] In this chemistry system the effect of unmixedness on individual reactions is modeled by decreasing any rate for which one or more of the species involved goes negative during fluctuation of its concentration about the average value. (Temperature fluctuations are not considered.)

In addition to calculations using Spiegler's system of 7 species and 8 reactions, calculations were also made using 12 species and 25 reactions. The latter system required the solution of twice as many differential equations for chemical species, but this was judged to be necessary in order to examine the effect of the added equations on the generation rates of radicals such as H, O, and OH. The elemental reactions by means of which H_2 and O_2 are transformed into H_2O provide multiple paths between the reactants and the product, most of which depend on the presence of high concentrations of radicals. The relative importance of the paths changes as conditions in the flow change, and it is important not to neglect any path which might be a large source or sink for one or more of the radicals, since such a path might be critical for prediction of ignition.

Description of Computer Program and Finite-Rate Chemistry

The two-dimensional, parabolic computer program is described in a previous report.[1] Solutions of parabolic partial differential equations for transport of momentum, energy, and mass are accomplished by the finite difference technique of Patankar and Spalding.[4] These equations are

$$\rho u\frac{\partial u}{\partial x}+\rho v\frac{\partial u}{\partial y}-\frac{1}{y^i}\frac{\partial}{\partial y}\left(\mu_t y^i\frac{\partial u}{\partial y}\right)=-\frac{\mathrm{d}p}{\mathrm{d}x} \tag{1}$$

$$\rho u\frac{\partial h}{\partial x}+\rho v\frac{\partial h}{\partial y}-\frac{1}{y^i}\frac{\partial}{\partial y}\left(\frac{\mu_t}{\sigma_h}y^i\frac{\partial h}{\partial y}\right)=-\frac{1}{y^i}\frac{\partial}{\partial y}\left\{y^i\left[\left(\frac{\mu_t}{\sigma_u}-\frac{\mu_t}{\sigma_h}\right)\frac{\partial}{\partial y}\left(\frac{u^2}{2}\right)+\left(\frac{\mu_t}{\sigma_k}-\frac{\mu_t}{\sigma_h}\right)\frac{\mathrm{d}k}{\mathrm{d}k}\right]\right\} \tag{2}$$

$$\rho u\frac{\partial a}{\partial x}+\rho v\frac{\partial a}{\partial y}-\frac{1}{y^i}\frac{\partial}{\partial y}\left(\frac{\mu_t}{\sigma_m}y^i\frac{\partial a}{\partial y}\right)=\dot{w} \tag{3}$$

where $i=0$ for plane flow, and $i=1$ for axisymmetric flow.

Presented as Paper 79-0355 at the AIAA 17th Aerospace Sciences Meeting, New Orleans, La., Jan. 15-17, 1979; submitted Feb. 12, 1979; revision received June 29, 1979.

Index categories: Combustion Stability, Ignition, and Detonation; Reactive Flows; Thermochemistry and Chemical Kinetics.

*Aerospace Engineer, Hypersonic Propulsion Branch, High-Speed Aerodyanmics Division.

Two more equations are solved for transport of turbulence kinetic energy k and of the dissipation rate of turbulence kinetic energy ϵ.

$$\rho u\frac{\partial k}{\partial x}+\rho v\frac{\partial k}{\partial y}-\frac{1}{y^i}\frac{\partial}{\partial y}\left(\frac{\mu_t}{\sigma_k}y^i\frac{\partial k}{\partial y}\right)=\mu_t\left(\frac{\partial u}{\partial y}\right)^2-\rho\epsilon \quad (4)$$

$$\rho u\frac{\partial \epsilon}{\partial x}+\rho v\frac{\partial \epsilon}{\partial y}-\frac{1}{y^i}\frac{\partial}{\partial y}\left(\frac{\mu_t}{\sigma_\epsilon}y^i\frac{\partial \epsilon}{\partial y}\right)$$

$$=C_{\epsilon 1}\left(\frac{\epsilon}{k}\right)\mu_t\left(\frac{\partial u}{\partial y}\right)^2-C_{\epsilon 2}\left(\frac{\epsilon}{k}\right)\rho\epsilon \quad (5)$$

Equations are also solved for the transport of fluctuations in fuel and oxidant.

$$\rho u\frac{\partial g_f}{\partial x}+\rho v\frac{\partial g_f}{\partial y}-\frac{1}{y^i}\frac{\partial}{\partial y}\left(\frac{\mu_t}{\sigma_{g_f}}y^i\frac{\partial g_f}{\partial y}\right)$$

$$=C_{g1}\left(\frac{\epsilon}{k}\right)\left(\frac{\partial u}{\partial y}\right)^2-C_{g2}\left(\frac{\epsilon}{k}\right)\rho g_f \quad (6)$$

$$\rho u\frac{\partial g_{ox}}{\partial x}+\rho v\frac{\partial g_{ox}}{\partial y}-\frac{1}{y^i}\frac{\partial}{\partial y}\left(\frac{\mu_t}{\sigma_{g_{ox}}}y^i\frac{\partial g_{ox}}{\partial y}\right)$$

$$=C_{g1}\left(\frac{\epsilon}{k}\right)\left(\frac{\partial u}{\partial y}\right)^2-C_{g2}\left(\frac{\epsilon}{k}\right)\rho g_f \quad (7)$$

Turbulence viscosity is computed from

$$\mu_t=C_\mu\rho k^2/\epsilon \quad (8)$$

The values of the constants used were those recommended by the authors of the paper from which the equations were taken.[5] These values are as follows:

$$C_\mu=0.09,\ C_{\epsilon 1}=1.43,\ C_{\epsilon 2}=1.92,\ C_{g1}=2.80,\ C_{g2}=2.00$$

$$C_{EBU}=0.53,\quad \sigma_u,\sigma_k=1.00,\quad \sigma_\epsilon=1.30,\quad \text{other } \sigma\text{'s}=0.70$$

The constants C_μ and $C_{\epsilon 2}$ are modified[5] for axisymmetric flow as follows:

$$C_\mu=0.09-0.04f \text{ and } C_{\epsilon 2}=1.92-0.0667f$$

Where

$$f=\left|\frac{Y}{2\Delta U}\left(\frac{\partial u_{cl}}{\partial x}-\left|\frac{\partial u_{cl}}{\partial x}\right|\right)\right|^{0.2}$$

Y is the radial width of mixing region, ΔU is the axial direction velocity difference across the width of mixing region, and u_{cl} is the axial velocity on centerline.

At Mach numbers above 1 a compressibility correction derived by Dash et al.[6] is applied. A factor whose magnitude varies from 1.00 at $M=1$ to 0.25 for large Mach number is multiplied by the turbulent viscosity as computed from the $k-\epsilon$ model. The correction factor is an empirical expression derived from experimental observations and is calculated as follows:

$$f_{cc}=0.25+0.75/\{1.0+\exp[24.73(M_T-0.2)]\} \quad (9)$$

where M_T is $k^{1/2}$ divided by the local speed of sound.

In the previous report[1] the chemical reaction term $\dot{w}$ in Eq. (3) was calculated using the equation

$$\dot{w}=-C_{\mathrm{EBU}}\rho g^{1/2}\left(\frac{\epsilon}{k}\right) \quad (10)$$

where ρ = density and g = mean square fluctuation in fuel or oxidant, whichever is smaller. The factor C_{EBU} was treated as an adjustable constant to enhance agreement with data, in contrast with the finite rate chemical reactions used here, which contained no adjustable constants. In this report, following Spiegler,[3] chemical changes are described by a set of N_R elementary reactions of the form

$$\sum_{j=1}^{N_S}\gamma'_{ij}M_j\underset{K_{bi}}{\overset{K_{fi}}{\rightleftharpoons}}\sum_{j=1}^{N_S}\gamma''_{ij}M_j,\quad i=1,2,\ldots,N_R \quad (11)$$

involving N_S species ($j=1,2,\ldots,N_S$). The reaction rates K_{fi} and K_{bi} are given by expressions of the form

$$K_i=A_iT^{Bi}e^{-C_i/T} \quad (12)$$

The rate of change of species j by reaction i is

$$(\dot{M}_j)_i=(\gamma''_{ij}-\gamma'_{ij})\left(K_{fi}\prod_{j=1}^{N_S}M_i^{\gamma'_{ij}}-K_{bi}\prod_{j=1}^{N_S}M_j^{\gamma''_{ij}}\right) \quad (13)$$

The total rate of change of species j is

$$\dot{M}_j=\sum_{i=1}^{N_R}(\dot{M}_j)_i \quad (14)$$

or

$$\dot{w}=\dot{M}_j\times(\text{molecular weight}) \quad (15)$$

To account for unmixedness, Spiegler replaced K_{fi} with $K_{fi}(1-U_{fi})$ and K_{bi} with $K_{bi}(1-U_{bi})$, where $0\leqq U_{fi}\leqq 1$ and $0\leqq U_{bi}\leqq 1$. The details of the procedure for calculating the U's are given in his report.[3] Briefly, rms values of concentration fluctuations are applied to time-averaged values of the species concentrations. The fraction of time that a species concentration has a negative value is used as the definition of the degree of unmixedness for that species. The largest value of unmixedness obtained when all species involved in a given reaction have been examined is used to compute the value of U_{fi} or U_{bi}.

The 8-reaction and the 25-reaction systems are described in Table 1. The first seven species listed and the reactions marked with an asterisk constitute the 8-reaction system; the remaining species and reactions are those added to test the importance of the extra reactions for obtaining accurate predictions. Reaction rates are also listed in Table 1.

The main difference between the 8-reaction and the 25-reaction system is the addition of HO_2 (hydroperoxyl), NO, and NO_2. Reactions involving HO_2 molecules are important for low temperature ignition studies, whereas NO and NO_2, which are found in most hot air test gases, sensitize H_2-air ignition at low temperature.[7]

Description of the Experimental Test Cases

The data of test case 1 were obtained by Beach.[1] In the experiment cold hydrogen ($T=251$ K) was injected along the axis of a circular supersonic stream of vitiated air ($T=1495$ K). (Vitiated air is obtained by burning hydrogen in air to obtain a hot gas mixture and then adding oxygen to obtain a test gas with 21% oxygen by volume.) The geometry and flow conditions are given in Fig. 1.

A similar experiment by Cohen and Guile[8] was chosen for test case 2. In their experiment, cold hydrogen ($T=276$ K) was injected into vitiated air ($T=1140$ K). Test case 2 is described in Fig. 2.

For the third case,[9] cold hydrogen ($T=254$ K) was injected into vitiated air ($T=1270$ K) from a two-dimensional slot in the wall of a wind tunnel. Test case 3 is described in Fig. 3.

Table 1 Species and reactions[a]

Species		Reactions			
1	H	1	$HNO_2 + M \rightarrow NO + OH + M$	14	$OH + OH \rightarrow H + HO_2$
2	O	2	$NO_2 + M \rightarrow NO + O + M$	15	$H_2O + O \rightarrow H + HO_2$
3	H_2O	*3	$H_2 + M \rightarrow H + H + M$	16	$OH + O_2 \rightarrow O + HO_2$
4	OH	*4	$O_2 + M \rightarrow O + O + M$	17	$H_2O + O_2 \rightarrow OH + HO_2$
5	O_2	*5	$H_2O + M \rightarrow OH + H + M$	18	$H_2O + OH \rightarrow H_2 + HO_2$
6	H_2	*6	$OH + M \rightarrow O + H + M$	19	$O + N_2 \rightarrow N + NO$
7	N_2	7	$HO_2 + M \rightarrow H + O_2 + M$	20	$H + NO \rightarrow N + OH$
8	N	*8	$H_2O + O \rightarrow OH + OH$	21	$O + NO \rightarrow N + O_2$
9	NO	*9	$H_2O + H \rightarrow OH + H_2$	22	$NO + OH \rightarrow H + NO_2$
10	NO_2	*10	$O_2 + H \rightarrow OH + O$	23	$NO + O_2 \rightarrow O + NO_2$
11	HO_2	*11	$H_2 + O \rightarrow OH + H$	24	$NO_2 + H_2 \rightarrow H + HNO_2$
12	HNO_2	12	$H_2 + O_2 \rightarrow OH + OH$	25	$NO_2 + OH \rightarrow NO + HO_2$
		13	$H_2 + O_2 \rightarrow H + HO_2$		

Reaction rates

	Forward rate constant[b]			Reverse rate constant[b]		
	A	B	C	A	B	C
1	5.0×10^{17}	−1.0	25000	8.0×10^{15}	0	−1000
2	1.1×10^{16}	0	32712	1.1×10^{15}	0	−941
3	5.5×10^{18}	−1.0	51987	1.8×10^{18}	−1.0	0
4	7.2×10^{18}	−1.0	59340	4.0×10^{17}	−1.0	0
5	5.2×10^{21}	−1.5	59386	4.4×10^{20}	−1.5	0
6	8.5×10^{18}	−1.0	50830	7.1×10^{18}	−1.0	0
7	1.7×10^{16}	0	23100	1.1×10^{16}	0	−440
8	5.8×10^{13}	0	9059	5.3×10^{12}	0	503
9	8.4×10^{13}	0	10116	2.0×10^{13}	0	2600
10	2.2×10^{14}	0	8455	1.5×10^{13}	0	0
11	7.5×10^{13}	0	5586	3.0×10^{13}	0	4429
12	1.7×10^{13}	0	24232	5.7×10^{11}	0	14922
13	1.9×10^{13}	0	24100	1.3×10^{13}	0	0
14	1.7×10^{11}	0.5	21137	6.0×10^{13}	0	0
15	5.8×10^{11}	0.5	28686	3.0×10^{13}	0	0
16	3.7×10^{11}	0.64	27840	1.0×10^{13}	0	0
17	2.0×10^{11}	0.5	36296	1.2×10^{13}	0	0
18	1.2×10^{12}	0.21	39815	1.7×10^{13}	0	12582
19	5.0×10^{13}	0	37940	1.1×10^{13}	0	0
20	1.7×10^{14}	0	24500	4.5×10^{13}	0	0
21	2.4×10^{11}	0.5	19200	1.0×10^{12}	0.5	3120
22	2.0×10^{11}	0.5	15500	3.5×10^{14}	0	740
23	1.0×10^{12}	0	22800	1.0×10^{13}	0	302
24	2.4×10^{13}	0	14500	5.0×10^{11}	0.5	1500
25	1.0×10^{11}	0.5	6000	3.0×10^{12}	0.5	1200

[a] The first 7 species and the starred reactions constitute the 8-reaction system. [b] Form of rate constant is $k = AT^B \exp(-C/T)$ with k in cm^3/mole-s or cm^6/$mole^2$-s.

For all the cases, the data used for comparison with calculated results were pitot pressure profiles and composition profiles. For test cases 1 and 2, profiles were measured at four axial distances from the injection point. For test case 3 the profiles of interest were measured at only one downstream location. Note that the limited number of test cases involve a range of air temperatures within which ignition phenomena would be expected to be important at the lower end and perhaps unimportant at the upper end.

Discussion of Results

For each case the experimentally determined distribution (derived from pitot pressure and composition profiles[1]) of mass flow is compared with calculated mass flow distributions obtained by assuming: 1) no reaction occurs; 2) all fuel and oxidant mixed is instantly reacted; or 3) reaction occurs through finite rate elemental reactions. Because of the change in density caused by heat release from chemical reactions, such plots are good indicators of the amount and location of reaction in a flow. Figures 4 and 5 give the results of this kind of comparison for test cases 1 and 2. For both cases the shifts of the curves in the radial direction due to heat release are clearly evident. The finite-rate results agree reasonably well with the data points for both cases, although agreement is better for test case 2. Comparison of the data with the no-reaction and equilibrium curves indicates that reaction for test case 1 began somewhere ahead of the first station at $x/d_j = 6.56$. The first indication of reaction for test case 2 is at $x/d_j = 17.8$, and even there the finite-rate curve, the no-reaction curve, and the data all lie close together. The conclusion drawn from this, and borne out by the later figures, is that ignition occurred early for test case 1 but was delayed for test case 2.

It should be pointed out that not all calculated results are shown on the figures. This was done to avoid putting a large number of nearly identical curves on a single figure. Comments are used to point out the nature of omitted curves. For example, the no-reaction curve is not shown for the first three stations of Fig. 5 because it coincided with the finite-rate curve. It is concluded that little or no reaction occurred for test case 2 within a distance of 18 diameters from the injection point.

Figures 6 and 7 show N_2 and O_2 profiles at four stations† downstream of injection. The N_2 curves show that the mixing predicted by the calculations is correct, because both the centerline values and the shapes of the curves agree well with the data. Since O_2 and N_2 are assumed to mix with the fuel in

†For test case 1, x/d_j values differ between Fig. 4 and Fig. 6 because the composition was sampled at stations slightly downstream of the pitot probes.

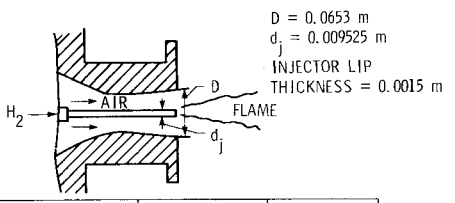

	HYDROGEN JET	FREE STREAM
MACH NUMBER, M	2.00	1.90
TEMPERATURE, T, K	251	1495
VELOCITY, u, m/s	2432	1510
PRESSURE, p, MPa	0.1	0.1
MASS FRACTION:		
a_{H_2}	1.000	0
a_{O_2}	0	0.241
a_{N_2}	0	0.478
a_{H_2O}	0	0.281

Fig. 1 Test case 1.

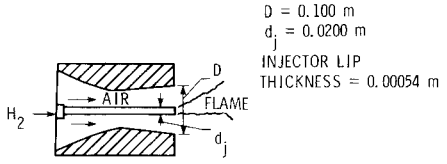

	HYDROGEN JET	FREE STREAM
MACH NUMBER, M	1.46	1.86
TEMPERATURE, T, K	276	1140
VELOCITY, u, m/s	1877	1265
PRESSURE, p, MPa	0.09	0.09
MASS FRACTION:		
a_{H_2}	1.0	0
a_{O_2}	0	0.260
a_{N_2}	0	0.590
a_{H_2O}	0	0.150

Fig. 2 Test case 2.

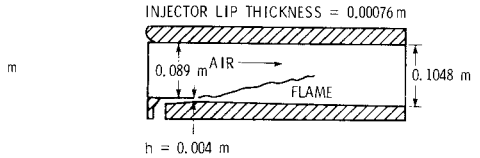

	HYDROGEN JET	FREE STREAM
MACH NUMBER, M	1.00	2.44
TEMPERATURE, T, K	254	1270
VELOCITY, u, m/s	1216	1764
PRESSURE, p, MPa	0.1	0.1
MASS FRACTION:		
a_{H_2}	1.000	0
a_{O_2}	0	0.258
a_{N_2}	0	0.486
a_{H_2O}	0	0.256

Fig. 3 Test case 3.

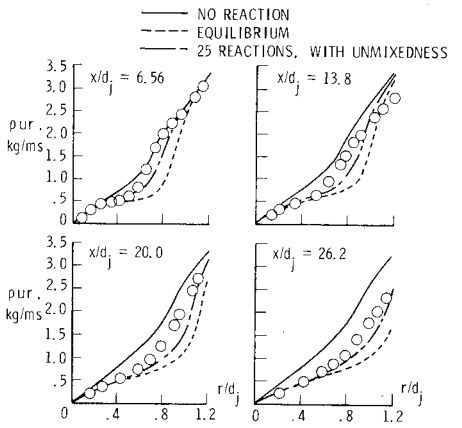

Fig. 4 Mass flow distributions for test case 1.

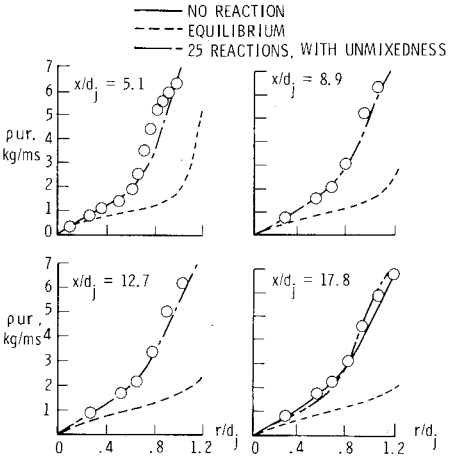

Fig. 5 Mass flow distributions for test case 2.

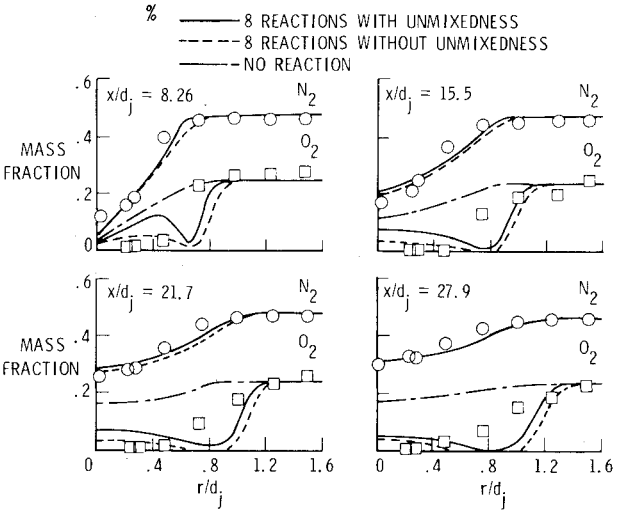

Fig. 6 N_2 and O_2 profiles for test case 1.

exactly the same way, the O_2 and N_2 curves will be similar in shape if no reaction occurs. This is true for the solid lines in Fig. 7, and the data at all stations agree with them. This observation reinforces the conclusion drawn from Fig. 5 that little or no reaction occurred for test case 2—at least as far downstream as $x/d_j = 17.8$. The no-reaction curves are omitted from Fig. 7 because they coincide with the finite-rate curves. They appear on Fig. 6 to show, through comparison with the finite-rate results, how much oxygen was consumed.

Figures 6 and 7 are used to illustrate two kinds of comparison calculations: a) reaction with and without unmixedness, and b) 25-reaction results versus 8-reaction results.

In every case calculated, except for one notable exception discussed later in the paper, the comparison between calculations made with and without unmixedness was as shown in Fig. 6. That is, the effect is not small enough to be negligible, but it does not change shapes and magnitudes much for flames already ignited. Although the curves are not shown, the calculated results for Fig. 6 were almost identical when the 25-reaction system was used instead of the 8-reaction system. It should be recalled that, because the air for test case 1 was hot (1495 K), ignition took place early.

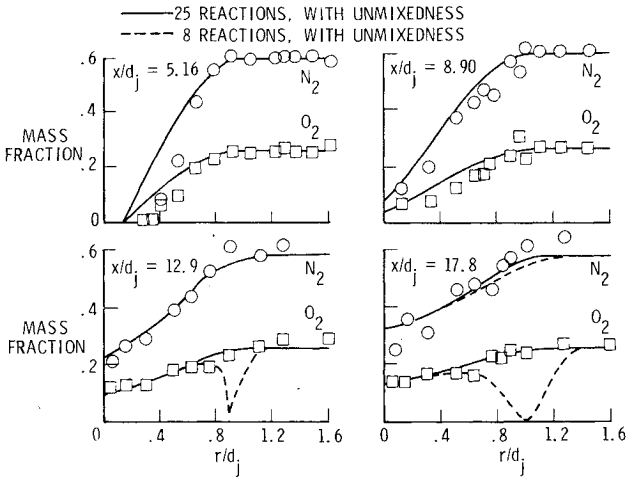

Fig. 7 N_2 and O_2 profiles for test case 2.

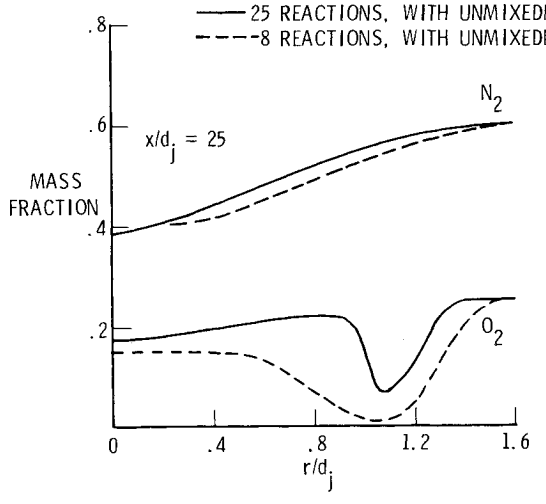

Fig. 8 Test case 2 profiles beyond the measured data.

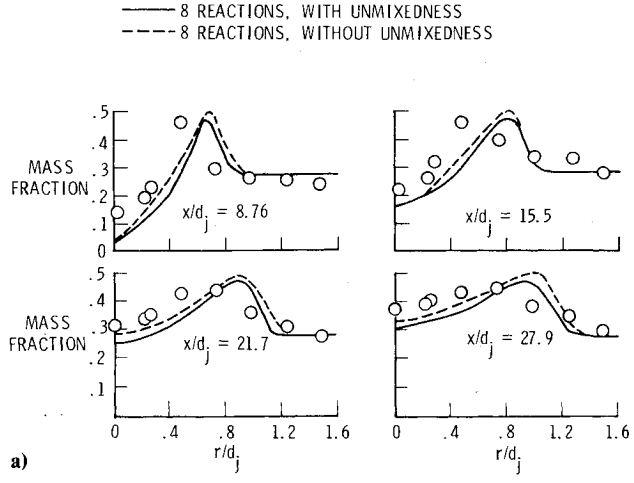

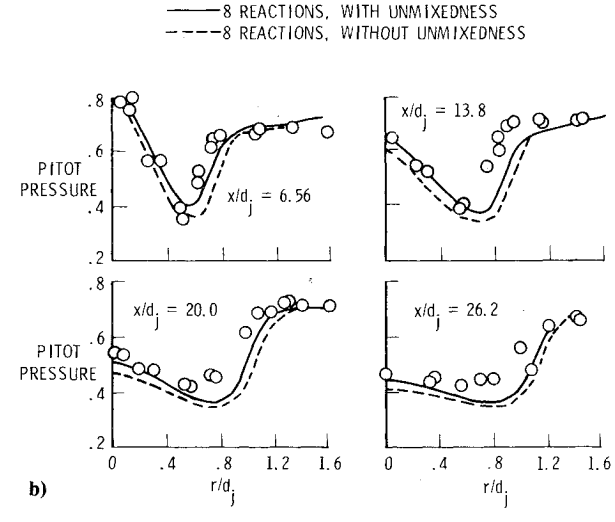

Fig. 9 Test case 1 profiles. a) H_2O mass fraction; b) pitot pressure.

The results of calculations for Fig. 7 were like those for Fig. 6 in that no important differences were found due to inclusion of the unmixedness equations. Thus the results obtained without unmixedness are not shown. The important differences for this case are between the results obtained using the different reaction systems. It was concluded earlier while discussing Fig. 5 that ignition did not occur for test case 2 using the 25-reaction system until at least $x/d_j = 17.8$, and that even then the indication was faint. The 8-reaction results shown in Fig. 7 predict the occurrence of ignition between $x/d_j = 8.90$ and $x/d_j = 12.9$. Obviously, the 25-reaction system does the better job for this test case.

Since there was a faint indication of ignition at $x/d_j = 17.8$, the calculation was extended to $x/d_j = 25$ with the results shown in Fig. 8. Ignition is predicted to occur between $x/d_j = 17.8$ and $x/d_j = 25$, and the results of the 25-reaction and the 8-reaction systems are beginning to resemble each other. Unfortunately, there are no data to compare with this calculation.

Figures 9 and 10 show H_2O profiles and pitot pressure profiles. For test case 1 the agreement between experiment and theory is reasonably good. The shapes of the curves resemble data point distribution shapes and the magnitudes are about right. The radial shifts in position of the calculated pitot pressures relative to the data indicate that more reaction was predicted than actually occurred. Examination in Fig. 6 of the relative positions of the data and the deep dips in the calculated O_2 curves reveals that indeed more O_2 was consumed in the calculated results than in the experimental results. The most likely cause for this discrepancy is thought to be incorrect temperature dependence for some of the reaction rates, leading to too rapid reaction as the temperature in the flame zone rises.

For test case 2 in Fig. 10, the agreement between theory and experiment is not as satisfying. There is no difficulty with the pitot pressure, since the previous conclusion that essentially no reaction took place is borne out here. However, there seems to be no way to reconcile with theory the apparent measurement of H_2O in excess of amounts which could have been transported from the vitiated air (thus implying reaction). All that can be said is that the majority of evidence points to no reaction.

Results for test case 3 are shown in Fig. 11. Finite-rate curves are plotted for 25 reactions, both with and without unmixedness. With unmixedness very little reaction occurred; without it, reaction was nearly complete at $x/d_j = 89$. With the 8-reaction system the results were nearly the same.

The data station is far downstream of the ignition point for either of the reaction systems. Thus, as in the test case 2 results, profiles are essentially identical for the two systems. The surprising result is the effect of unmixedness. In Eq. (12) unmixedness decreases the magnitudes of K_{fi} and K_{bi}. For this test case, conditions were such that the decrease in reaction rates caused by applying the unmixedness correction was critical to ignition, with the result that ignition was suppressed when the unmixedness correction to the reaction rates was

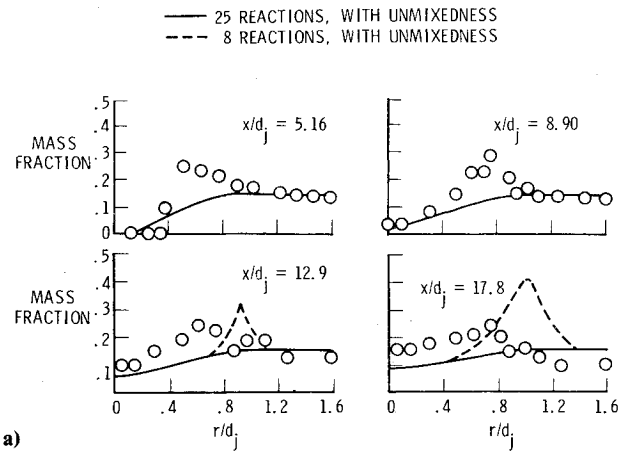

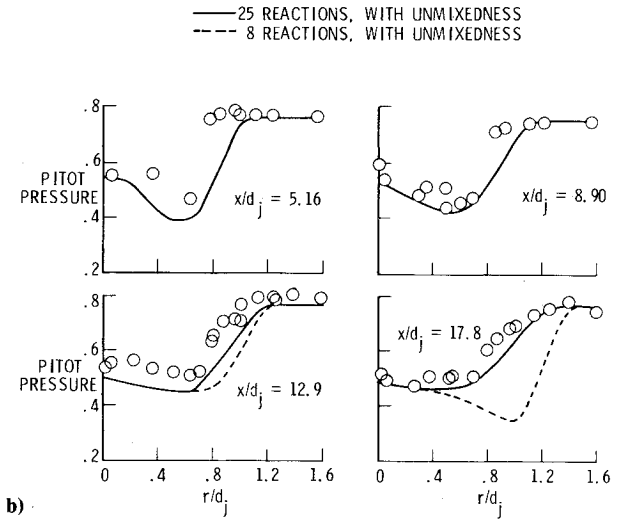

Fig. 10 Test case 2 profiles. a) H_2O mass fraction; b) pitot pressure.

included. Because of the special conditions present in this case, no great importance is attached to the fact that the chemistry model without unmixedness produced results which agree so much better with data than did the model with the unmixedness correction. In fact, the only case presented here which allows comparison with data of the chemistry model with and without the unmixedness correction is test case 1, and there the effect does not appear to be large.

Concluding Remarks

The foregoing discussion of results demonstrates that a combined finite-rate chemistry/unmixedness model can provide a viable tool for analyzing hydrogen/air supersonic flames. All calculations were carried out with fixed constants in the mixing and chemistry models, in contrast to the prior work using an eddy breakup model in which large adjustments of a parameter were necessary. Ignition characteristics of the flames were found to be sensitive both to the chemical kinetics and to the unmixedness correction.

The principal conclusions reached from the work reported here are:

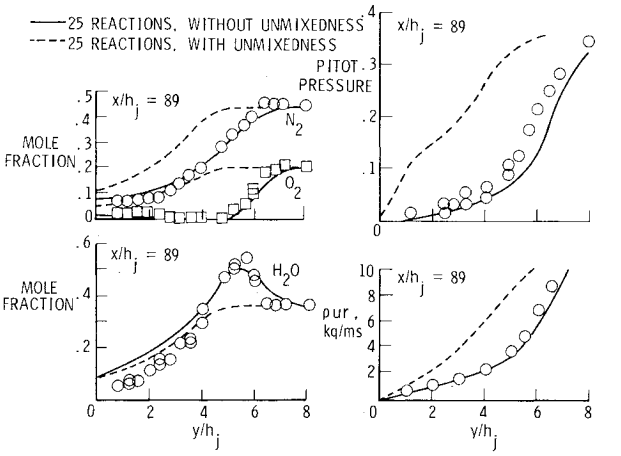

Fig. 11 Profiles for test case 3.

1) The 25-reaction system is superior to the 8-reaction system for prediction of ignition. This is attributed to the presence of adequate reaction paths to provide sources and sinks for free radicals such as H, O, and OH.

2) Once ignition occurs, the 8-reaction system results are as good as those from the 25-reaction system. In a system where external means for ignition are provided or where spontaneous ignition is known to be fast, the 8-reaction system should be adequate.

3) With one exception, corrections to the reaction rates to account for unmixedness in turbulent flows at the molecular level produced changes in the computed results which were too large to be neglected, but were too small to change the general shape and magnitude of the computed curves. In the exceptional case unmixedness made a major difference, for including its effect on the reaction rates caused the fuel mixture to fail to ignite.

References

[1] Evans, J. S., Schexnayder, C. J., Jr., and Beach, H. L., Jr., "Application of a Two-Dimensional Parabolic Computer Program to Prediction of Turbulent Reacting Flows," TP-1169, NASA, 1978.

[2] Lilly, D. G., "Turbulent Swirling Flame Prediction," *AIAA Journal*, Vol. 12, Feb. 1974, pp. 219-223.

[3] Spiegler, E., Wolfshtein, M., and Manheimer-Timmat, Y., "A Model of Unmixedness for Turbulent Reacting Flows," *Acta Astronautica*, Vol. 3, 1976, pp. 265-280.

[4] Patankar, S. V. and Spalding, D. B., *Heat and Mass Transfer in Boundary Layers*, 2nd ed., International Textbook Co., Ltd., London, 1970.

[5] Launder, B. E., Morse, A., Rodi, W., and Spalding, D. B., "Prediction of Free Shear Flows—A Comparison of Six Turbulence Models," Vol. 1, Paper No. 5, SP-321, NASA, 1973.

[6] Dash, S., Weilerstein, G., and Vaglio-Laurin, R., "Compressibility Effects in Free Turbulent Shear Flows," TR-75-1436, AFOSR, Aug. 1975.

[7] Slack, M. and Grillo, A., "Investigation of Hydrogen-Air Ignition Sensitized by Nitric Oxide and by Nitrogen Dioxide," CR-2896, NASA, 1977.

[8] Cohen, L. S. and Guile, R. N., "Investigation of the Mixing and Combustion of Turbulent, Compressible Free Jets," CR-1473, NASA, 1969.

[9] Burrows, M. C. and Kurkov, A. P., "Analytical and Experimental Study of Supersonic Combustion of Hydrogen in a Vitiated Air Stream," TM X-2828, NASA, 1973.